JOURNAL OF GEOPHYSICAL RESEARCH, VOL. 98, NO. C9, PAGES 16,379–16,385, SEPTEMBER 15, 1993

Effects of Westerly Wind Bursts Upon the Western Equatorial Pacific Ocean, February–April 1991

THIERRY DELCROIX AND GÉRARD ELDIN

Groupe Surtropac, Centre ORSTOM de Nouméa, Nouméa, New Caledonia

MICHAEL MCPHADEN

Pacific Marine Environmental Laboratory, National Oceanic and Atmospheric Administration, Seattle, Washington

ALAIN MORLIÈRE

ORSTOM/LODYC, Université Pierre et Marie Curie, Paris, France

In February–April 1991, episodes of 2 to 8 m s^{-1} westerly winds of 3 to 11 days' duration occurred in the western Pacific warm pool. Resulting modifications of the upper ocean in current and hydrology are quantified using data from an equatorial mooring at 165°E and from three cruises within 30 days of one another along 165°E. During westerly wind bursts (WWB) stronger than 4 m s^{-1}, the upper 50 m becomes isothermal to within 0.1°C and sea surface temperature (SST) drops by 0.3–0.4°C between 5°S and 2.5°N. Conversely, SST starts warming and the upper 50 m restratifies in 4–5 days after the end of WWB. In contrast to previous observations, salinity between 0 and 50 m appears almost unaffected by WWB; it freshens by 0.4 practical salinity unit in March within an area of 1°–2° of latitude around the equator but not necessarily in direct response to WWB. As for zonal circulation, surface equatorial flow accelerates eastward 2–3 days after the beginning of westerlies. Then, after less than 2 weeks, eastward and westward jets both develop from 2°N to 2°S in the upper and lower halves of the temperature mixed layer, respectively. Changes in zonal mass transport in this layer were as much as 30 Sv between 2.5°S and 2.5°N from one cruise to the next.

1. INTRODUCTION

Together with the seasonal monsoon reversal, episodes of westerly wind bursts (WWB) are prominent aspects of wind variability in the western Pacific warm pool [*Wyrtki and Meyers*, 1976; *Luther et al.*, 1983]. Analysis of wind records derived from island stations situated near the international date line has revealed that WWB last for only a few days, may have amplitudes in excess of 10 m s^{-1}, and have typical meridional and zonal scales of 3°–5° of latitude and 10°–30° of longitude [e.g., *Harrison and Giese*, 1991]. On a seasonal time scale, WWB tend to be more frequent from November to April, a season during which cyclone pairs astride the equator can result in very strong westerly winds [*Keen*, 1982]. On an interannual time scale, the highest probability of WWB occurrence exists very close to the equator, where about 80% of WWB happen during El Niño–Southern Oscillation (ENSO) periods.

The relative frequency of WWB contributes greatly to the apparent low-frequency reduction in the zonal wind known to characterize canonical ENSO [*Wyrtki*, 1975; *Rasmusson and Carpenter*, 1982; *Luther et al.*, 1983]. Theoretical and modeling studies also indicated that ENSO-related warming of eastern Pacific sea surface temperature (SST) could be caused by Kelvin wave response to westerly wind events [*Philander*, 1981; *Harrison and Schopf*, 1984; *Giese and Harrison*, 1990]. Hence WWB were suspected to be an important part of the physics governing the coupled ocean-atmosphere ENSO phenomenon. The precise role of WWB forcing in the ENSO phenomenon is, however, not clearly understood and is still a matter of debate.

Local effects of WWB on current structures have long been documented through various types of observations. *Hisard et al.* [1970] presented remarkable results of an investigation of the March–April 1967 variability in equatorial currents at 170°E. Although near-surface eastward equatorial flows had already been reported in the literature [e.g., *Yoshida et al.*, 1959; *Istoshin and Kalashnikov*, 1965], Hisard et al. were the first to associate WWB and the appearance above the main thermocline of an eastward zonal current (2°S to 2°N; 20–30 cm s^{-1}) above a westward counterflow (40 cm s^{-1}). More recently, near-surface eastward flows (2°S to 2°N; 40–110 cm s^{-1}) have been observed at 165°E during westerly wind episodes in January 1985, 1987, and 1989 and in December 1986 [*Delcroix et al.*, 1987, 1992; *Eldin*, 1987, 1989]. Aside from discrete observations, the temporal evolution of current structures in response to WWB were further documented from moored data at 0°–165°E [*McPhaden et al.*, 1988, 1990, 1992]. For example, within a week of westerlies in November 1989, the westward zonal current reversed to reach speeds in excess of 1 m s^{-1}. Interestingly, the upper 100 m became isothermal to within 0.1°C, and the salinity field underwent a dramatic drop of 1 practical salinity unit (psu).

At 165°E, equatorially trapped eastward currents were also observed outside of the normal cyclone season. In May 1986, unusual eastward currents (>1 m s^{-1}) were clearly linked to WWB associated with a tropical cyclone pair [*McPhaden et al.*, 1988]. In July 1987, eastward flows (>1 m

Paper number 93JC01261.
0148-0227/93/93JC-01261$05.00

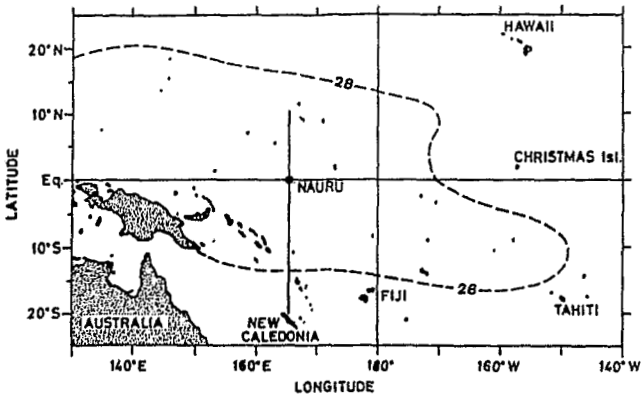

Fig. 1. Locations of temperature, salinity, and ADCP sections (solid line) and of the equatorial mooring at 165°E (circle). Overplotted is the climatological mean position of the 28°C surface isotherm (broken line) as derived from *Levitus* [1982].

s^{-1}) reflected the combined effects of local (WWB) and remote forcing, the latter in a form of a first-meridional, first-baroclinic-mode upwelling equatorial Rossby wave propagating from the eastern Pacific [*Delcroix et al.*, 1992].

Despite the published literature dealing with WWB, our knowledge of the effects of WWB on the western equatorial Pacific is far from satisfactory. Indeed, describing, understanding, and ultimately predicting the oceanic response to wind stress forcing in the western Pacific warm pool are major objectives of the international Tropical Ocean–Global Atmosphere Coupled Ocean-Atmosphere Response Experiment (TOGA COARE) program [*World Climate Research Program*, 1990]. In line with these objectives, the purpose of this work is to document the local oceanic response to WWB occurring in the western equatorial Pacific for February–April 1991. For this, we use three main sources of data: first, three hydrographic and acoustic Doppler current profiling (ADCP) sections along 165°E, separated in time by 10–20 days; second, a current meter mooring at 0°–165°E; third, the Nauru island wind station (1°S, 167°E). Data collection and processing are discussed in section 2. Description of the wind forcing is then given in section 3. In section 4, emphasis is placed on the local oceanic response to WWB. Conclusions and discussion are presented in the last section.

2. DATA

The primary data sets we use are shipboard and mooring measurements along 165°E (Figure 1.) Shipboard measurements were collected during the Alize 2 and Surtropac 14 cruises on board the R/V *Le Noroit*. Standard hydrographic observations were made with Neil-Brown Mark III (Alize 2) and SeaBird SBE-9 (Surtropac 14) conductivity-temperature-depth (CTD) instruments. Each expedition obtained vertical profiles of temperature and salinity at selected latitudes ranging from 20°S to 8°N. Hydrographic casts were made down to at least 1000 dbar and processed to a 2-dbar vertical resolution. Corrections of salinity profiles were based on rosette sampling and laboratory calibrations. Specifics of CTD data acquisition and processing procedures are discussed by *Reverdin et al.* [1991] and *Delcroix et al.* [1991*a*].

During the cruises, sea surface temperature and salinity (hereinafter referred to as SST and SSS) were measured at about 3.5-m depth using a SeaBird SBE-21 Seacat instrument connected to a shipboard drain pumping water at 4.5 L/min. SST and SSS were recorded every 5 min together with the Global Positioning System (GPS) position. Along 165°E, this results in a 1.2-km meridional resolution, given the 4 m s^{-1} average ship speed, including stops for CTD stations and mooring deployments. Laboratory calibrations of temperature and conductivity sensors were performed in May 1990 by SeaBird, Inc. In addition, SST and SSS were compared to simultaneous 2-dbar CTD measurements; for the 64 comparisons made, means ± root-mean-square (rms) differences (CTD minus thermosalinograph) were -0.17 ± 0.13°C and 0.02 ± 0.02 psu. Further information is given by *Grelet et al.* [1992].

Shipboard ADCP data were also obtained during the Alize 2 and Surtropac 14 cruises with an RD Instruments 153.6-kHz profiler. Version 2.48 of RDI Data Acquisition Software was programmed for a bin width and a pulse length of 8 m. Velocity profiles were vector averaged in 5-min ensembles. Absolute velocities were estimated by combining GPS navigation and ship-relative ADCP measurements, leading to a maximum error of 5-7 cm s^{-1} [*Bahr et al.*, 1989]. Details of ADCP data processing are given by *Eldin* [1991], *Eldin et al.* [1992], and *Delcroix et al.* [1991*a*] for the Alize 2 and Surtropac 14 cruises, respectively. Note that the shallowest ADCP measurements (16 m) were extrapolated up to the surface for current transport calculation.

Temperature and current were measured at 0°–165°E from a taut-line surface mooring with an EG&G vector-measuring current meter at 10 m and with six model 610 EG&G vector-averaging current meters evenly spaced between 50 and 300 m. Temperature and salinity were measured at additional depths with SeaData temperature recorders and SeaBird SBE-16 Seacat conductivity and temperature recorders; only measurements at 3, 11, 30, and 51 m are considered here. Accuracies are a few cm s^{-1} for current speeds, 0.01°C for temperatures, and 0.02–0.03 psu for salinities. Data were internally recorded at intervals of 15 min to 1 h, depending on instrument type. Detailed information on instrument accuracies and data processing is given by *Feng et al.* [1991].

The large-scale wind field was derived from the Florida State University analysis. Pseudo stress vectors (units of m^2 s^{-2}) are available on a 2° latitude by 2° longitude grid on a monthly basis [*Goldenberg and O'Brien*, 1981]. Because of instrument failure, wind records are not available at the 0°, 165°E, mooring location in February and March 1991. Therefore measurements from Nauru island (1°S, 167°E) are used instead. Between March 1989 and July 1991, the cross correlation of 455 concurrent records of daily zonal wind components at 0°, 165°E, and Nauru was 0.90 with a mean and rms difference (0°, 165°E, minus Nauru) of −0.1 and 1.4 m s^{-1}, respectively. Also, eastward wind components recorded at 0°, 165°E, exist 80% of the time at Nauru island (85 of 106 days), with a mean and rms difference (0°, 165°E, minus Nauru) of 0.4 and 1.5 m s^{-1}, respectively. Thus zonal winds at Nauru are reasonably representative of those at 165°E, although in our data set, there is a tendency for Nauru westerlies to be slightly weaker and of shorter duration than those at the mooring sites. These small differences will not affect our main conclusions.

3. WIND FORCING

To set the context, the large-scale wind field is shown in Figure 2 for February and March 1991. West of 165°E, in February, NE and SE trade winds are found north of the equator and south of 10°S, respectively. In between, the seasonal NW monsoon appears slightly enhanced. In March, SE trade winds intensify, NE winds change to NNE, and westerly winds appear south of 2°N extending to the South Pacific Convergence Zone. East of 165°E, the trade winds exist both in February and March. On a monthly time scale, the 165°E longitude roughly delineates westward from eastward zonal wind components, suggesting possible wind reversals on this meridian on a shorter time scale. Interestingly, a comparison with Florida State University climatology data has shown that the trades and the NW monsoon were stronger than normal for the period in question.

Time series of zonal wind component recorded at Nauru island (Figure 3) and 0°–165°E reveal the occurrence of several WWB during February–March 1991. A first WWB appears from February 25 to March 7 (11 days), with an average zonal component of 2.5 m s^{-1}. (Note that the 1-day weak WWB in February 9 is not considered here.) A second WWB having a peak amplitude of 8.2 m s^{-1} occurs from March 16 to 19 (4 days), with an average of 6.2 m s^{-1}. Then, third and fourth WWB occur from April 3 to 5 (mean, 1 m s^{-1}) and April 20 to 24 (mean, 1.9 m s^{-1}), respectively; these last two WWB were also recorded by the newly deployed 0°–165°E mooring anemometer.

ATLAS mooring wind measurements along 165°E (not shown here) indicate that neither of these WWB is symmetrical about the equator. At 5°S, westerly wind is nearly continuous from February 8 to March 20. The first WWB lasts only 2 days at 2°N and does not reach 5°N, while the second one lasts 4 days at 2°N and 2 days at 5°N. For the February–April 1991 period, inspection of daily surface streamline analyses, provided by the Australian Bureau of Meteorology, shows that the first WWB is associated with tropical cyclone Kelvin, located in the southern hemisphere, while the second WWB is linked to a severe tropical strom, Tim, in the northern hemisphere. These two WWB are thus associated with successive enhanced cyclonic circulation in each hemisphere.

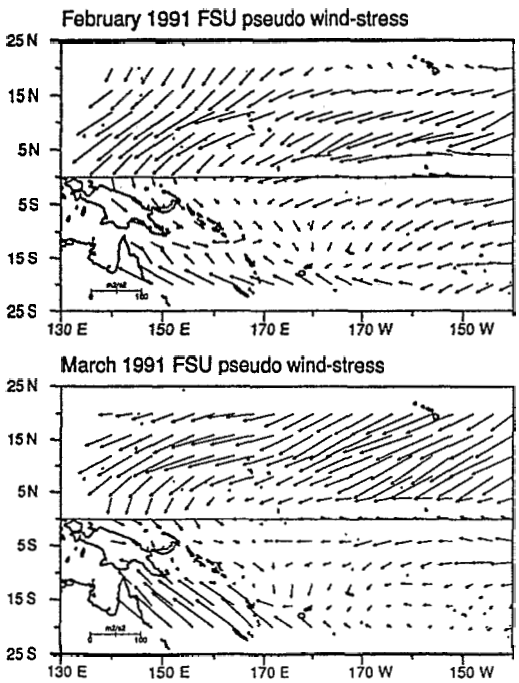

Fig. 2. Pseudo wind stress (m^2 s^{-2}) in February and March 1991 from Florida State University analysis averaged on a 4° × 4° grid.

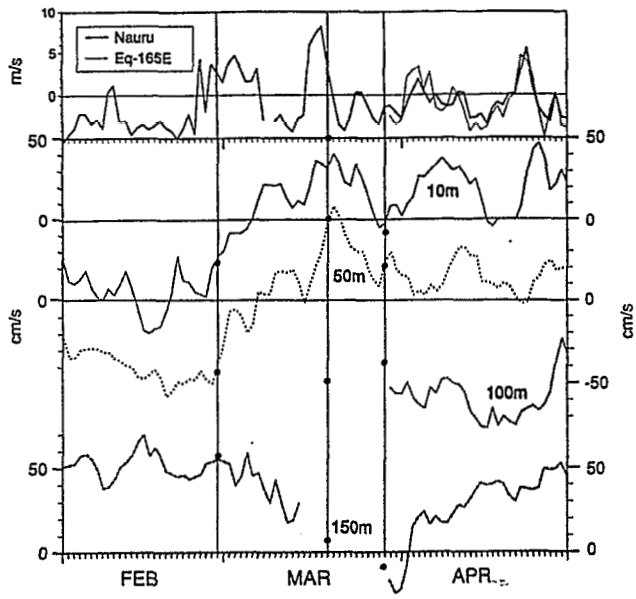

Fig. 3. Time series of (top) daily zonal wind components recorded at Nauru island (1°S, 167°E) and 0°, 165°E, and (bottom) daily zonal current components at 0°–165°E. Positive zonal components are directed eastward. Vertical bars indicate equatorial crossings of R/V *Le Noroit* during the Alize 2 and Surtropac 14 (legs 1 and 2) cruises. Shipboard ADCP measurements of zonal currents (black dots) at 16, 50, 100, and 150 m are included for comparison.

4. LOCAL RESPONSE

4.1. *Zonal Circulation*

Current measurements derived from continuous time series at 0°, 165°E, and three meridional ADCP sections along 165°E allow a description of zonal circulation changes in response to local WWB.

Time series of zonal currents for the equatorial mooring are presented in Figure 3. In February 1991, the South Equatorial Current (SEC) appears at 10 and 50 m, with westward speeds of 40–60 cm s^{-1}. At 150-m depth is the Equatorial Undercurrent (EUC) flowing eastward at 40–70 cm s^{-1}. Zonal currents at 10 and 50 m start to decrease noticeably on February 28, 2-3 days after the onset of the first WWB recorded at Nauru. This decrease occurs when the Alize 2 cruise crosses the equator, sailing southward.

During Alize 2, the well-known picture of zonal circulation in the western equatorial Pacific is observed (Figure 4). At depth, the EUC is centered very close to the equator at 190 m, with a 70 cm s^{-1} core velocity slightly above normal. The EUC transport within 2.5°N to 2.5°S is 25.4 Sv. Above the EUC is a well-developed SEC extending at least from 2.5°N to 7°S; its transport within 2.5°S to 2.5°N is −32.3 Sv. Velocity maxima of the SEC (> 40 cm s^{-1}) are located in the upper 120 m and north of 4°S. Two velocity cores faster than

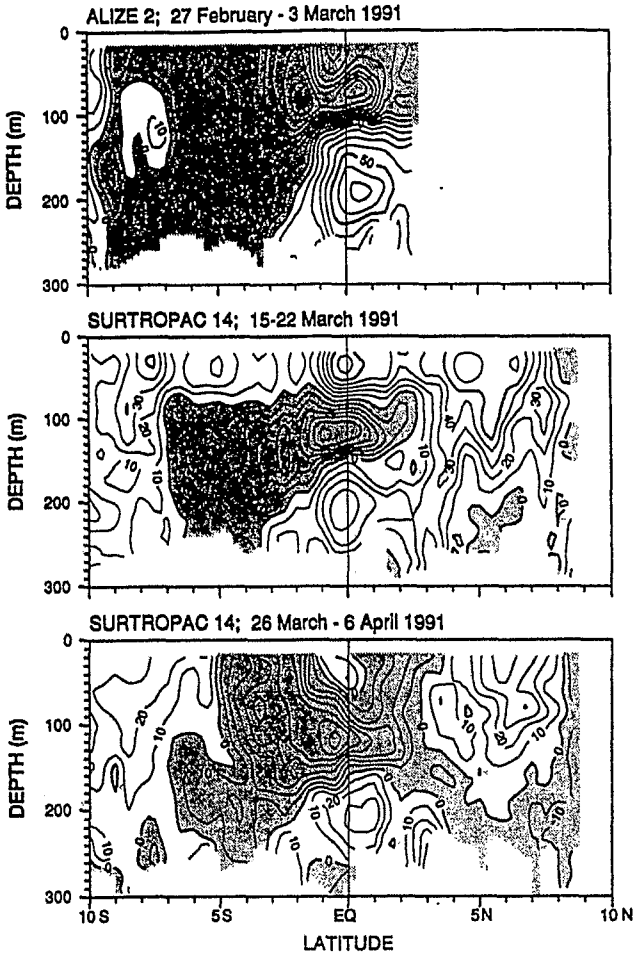

Fig. 4. Sections of absolute zonal currents (cm s^{-1}) at 165°E as measured during the cruises (top) Alize 2, (middle) Surtropac 14, leg 1, and (bottom) Surtropac 14, leg 2. Shaded areas denote westward flows.

70 cm s^{-1} are found near 70-m depth at 2°S and 1°N. In between is a near-surface relative velocity minimum which probably reflects the early effects of the first WWB on zonal circulation. Note that in the southern hemisphere, the South Equatorial Countercurrent lies from 7°S to 10°S and transports 5.5 Sv to the east.

The 10-m zonal current at the equator decelerates from February 28 and turns eastward after 10 days of westerly winds associated with the first WWB (Figure 3). Currents at 50-m depth undergo similar changes but lag behind the one at 10 m by 1–2 days. After the end of the first WWB, these near-surface eastward equatorial flows persist for 1 week of easterly wind, tending to decelerate eastward. Then they reach speeds faster than 40 cm s^{-1} on March 19, 2–3 days after the maximum westerly winds associated with the second WWB. At this time, the meridional extent of such eastward currents can be depicted by the ADCP data collected during the Surtropac 14 cruise sailing northward (leg 1).

Surtropac 14 leg 1 crosses the equator on March 19, 1 day after peak eastward wind associated with the second WWB. For this leg, eastward flows extend from 11°S to 7°N in the upper 70 m and are deeper than 200 m poleward of 2°N and 7°S (Figure 4). Of most interest are the modifications of zonal current structure near the equator compared with that determined during Alize 2. Indeed, an equatorially trapped eastward jet, consistent with the equatorial mooring data, now appears between 2.5°N and 2.5°S in the upper 70 m. This jet reaches speeds in excess of 50 cm s^{-1} and transports 11.7 Sv to the east. Below this eastward jet, in the 70- to 150-m depth range, an equatorially trapped westward jet shows up with a maximum speed of 60 cm s^{-1}; its transport between 2.5°N and 2.5°S is 11.7 Sv to the west. Still below is the eastward flowing EUC, whose upper limit deepens by 40 m and whose core speed (40 cm s^{-1}) and transport within 2.5°N-2.5°S (11.5 Sv) diminish by about 50% compared to the Alize 2 values.

Conceptual models of the equatorial mixed layer [e.g., *Stommel*, 1960; *Gill*, 1971; *McCreary*, 1985] may explain the alternation of equatorially trapped eastward and westward zonal jets observed in the upper 150 m. *McPhaden et al.* [1988] have explored a simplified model on the equatorial β plane for understanding the response of the upper layer to impulsive wind forcing such as WWB. For linear motion in a mixed layer of constant density and depth, a parabolic shear profile with a current reversal near the middle of the mixed layer develops in their model. This is in fair agreement with our measurements.

The 0°, 165°E, current measurements (Figure 3) indicate that eastward flows observed at 10- and 50-m depths during leg 1 of Surtropac 14 persist until the end of April 1991. These flows have a tendency to decrease during easterly wind periods and to accelerate eastward on two occasions 1–2 days after the third and fourth WWB. The meridional structure of the zonal current undergoes significant changes during leg 2 of Surtropac 14 (Figure 4) compared to leg 1, i.e., after 8 days of easterly wind. When leg 2 of Surtropac 14 crosses the equator on March 28, the SEC is back again from 5°S to 3°N (35.5 Sv between 2.5°N and 2.5°S) except at the equator, where a patch of eastward flow (1.8 Sv) persists. The equatorially trapped westward jet is still present, suggesting a slower response of the deep structure to the local wind forcing. Comparisons of the three cruise surveys show that changes in zonal transport above the main thermocline from one cruise to the next are 30 Sv between 2.5°S and 2.5°N.

4.2. *Hydrological Structures*

As for the zonal circulation, the description of changes in hydrological structure in response to WWB forcing benefits from complementary shipboard and moored measurements.

Moored time series measurements of temperature and salinity in the upper 51 m at 0°, 165°E, are presented in Figure 5. In February 1991 the equatorial temperature and salinity structures undergo wide variations near the surface. In particular, the SST varies from 29.7°C to 30.3°C on a weekly time scale, and the salinity rises by 0.5–0.7 psu in the upper 0–50 m between February 18 and 26. For perspective, it should be kept in mind that these variations occur prior to the WWB.

By the end of February 1991, SST and SSS at the equator are near 30°C and 34.8 psu, respectively. SST is about 1°C warmer than normal, whereas SSS falls within 0.05 psu of the mean climatological conditions [*Delcroix et al.*, 1992]. When the Alize 2 cruise crosses the equator on February 28, SST warmer than 30°C is found within 2.5° latitude of the

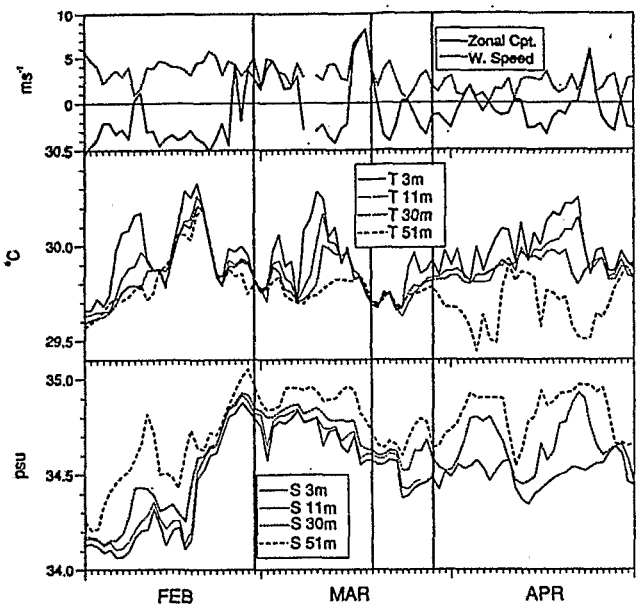

Fig. 5. Time series of (top) daily zonal wind components (positive eastward) and wind speed recorded at Nauru island (1°S, 167°E), (middle) daily temperature measurements at 0°, 165°E, and (bottom) daily salinity measurements at 0°, 165°E. Vertical bars are as in Figure 3.

equator (Figure 6), and the 29°C surface isotherm extends poleward of 2.5°N to 17°S. The meridional extent of SST > 29°C as well as its zonal extent (*Climate Diagnostic Bulletin*, National Meterological Center, Washington, D. C., 1991) is exceptionally large and corresponds to a pre-ENSO situation.

In March–April 1991, the equatorial near-surface temperature appears to be directly influenced by WWB (Figure 5). After the beginning of each WWB stronger than 3–4 m s^{-1}, the SST cools by 0.3–0.4°C and the upper 50 m becomes isothermal to within 0.1°C. Conversely, following the end of each WWB, the SST starts warming and the upper 50 m restratifies in 4–5 days. A period of low wind speed is evident after the end of the second WWB, from March 19 on. Then, the 0- to 50-m equatorial temperature stratifies, and the SST warms almost linearly by about 0.5°C in 1 month (Figure 5). These observations corroborate the possible role of mixing and/or evaporative cooling in temperature changes of the upper 50 m [*Meyers et al.*, 1986; *McPhaden and Hayes*, 1991].

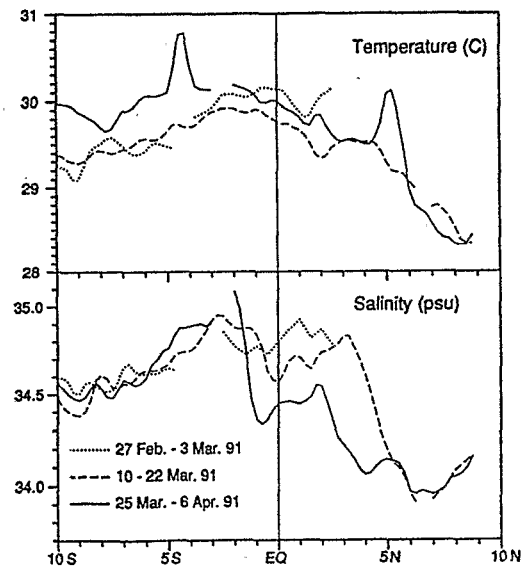

Fig. 6. Sections at 165°E of (top) sea surface temperature and (bottom) sea surface salinity during cruises Alize 2 (February 27–March 3, 1991; dotted line), Surtropac 14 leg 1 (March 10–22, 1991; broken line), and Surtropac 14 leg 2 (March 25–April 6, 1991; solid line). The 5-min thermosalinograph data have been smoothed with a 1-h median filter and gridded every 0.25° of latitude except for 2.5°N to 2.5°S salinity data for the Alize 2 cruise, which come from a CTD probe.

SST measured during Surtropac 14, leg 1 (Figure 6), provides information about the meridional extent of the SST cooling. The surface cooling associated with the second WWB ranges in latitude from 5°S northward to 2.5°N, with a drop of 0.3°C between 2.5°N and 2.5°S compared with values determined during Alize 2. Ten days after the second WWB, during Surtropac 14, leg 2, SST has risen by 0.2°C (2.5°N to 2.5°S), which is consistent with the equatorial mooring data. For the analyzed period, it is interesting to note that equatorial SST cooling and upper layer homogenization are of the same order of magnitude as observed in May 1986 and November 1989 [*McPhaden et al.*, 1988, 1992]. These three results, indicating only modest cooling, differ markedly from the 1.2°C SST cooling associated with a WWB event in January 1986 at 143°–150°E [*Lukas and Lindström*, 1991].

In contrast to temperature, the influence of WWB on salinity in the surface layer is not so obvious. Figure 5 indicates a slight tendency for salinity to become uniform in the upper 50 m 2–3 days after maximum westerly wind associated with the second and last WWB. Conversely, salinity stratification tended to increase during the first WWB. On a longer time scale than for WWB, the 0- to 50-m layer salinity is well mixed in March and restratifies in April. These last 2 months correspond to periods of high and low wind speeds, respectively, suggesting the possible role of vertical mixing in surface layer salinity stratification.

SSS measured along 165°E (Figure 6) confirms the decrease (0.4 psu/month) observed in March at the equatorial mooring location. It indicates that the SSS freshening extends meridionally from 5°N to 1.5°S. Within 2.5°N—2.5°S, the mean SSS decreases are 0.06 and 0.23 psu between Alize 2 and leg 1 of Surtropac 14 and between legs 1 and 2 of Surtropac 14, respectively. In the equatorial band, the SSS is thus weakly modified by WWB, in marked contrast to the November 1989 situation, when the salinity field in the surface layer drops by 1 psu immediately after the onset of westerlies. The weakness of the meridional gradient of SSS around the equator in March–April 1991 (Figure 6) compared with the November 1989 gradient [*McPhaden et al.*, 1992] may explain this difference.

Time series of subthermocline temperature at 0°, 165°E, and deep CTD measurements along 165°E (not shown here) do not indicate close relationships with WWB, At the equator, isotherms within the thermocline (20–25°C) steadily deepen by about 30 m from the end of February to early April. Along 165°E, the 0/1000 dbar dynamic height anomalies increase by 12 dyn cm within 2.5°N to 2°5°S between Alize 2 and leg 2 of Surtropac 14. This increase shows that changes induced by WWB in the surface layer are superim-

posed on low-frequency variations detected in subsurface temperature measurements.

5. Conclusions and Discussion

In February–April 1991, episodes of 2 to 8 m s^{-1} westerly winds of 3 to 11 days' duration occurred in the western Pacific warm pool a few months before warm ENSO anomalies developed in the eastern equatorial Pacific. The resulting local modifications of the upper ocean were quantified from temperature, salinity, and current data sets. This was made possible in the time domain from continuous measurements derived from an equatorial mooring at 165°E and in the space domain from three separate shipboard surveys along 165°E.

Overall, the local response of the WWB resembles that previously described for different periods and locations. Westward surface equatorial flows first decelerate 2–3 days after the onset of westerlies. After less than 2 weeks, equatorially trapped eastward and westward jets develop in the upper and lower halves of the temperature mixed layer, respectively. These two jets have a meridional scale of about 2° latitude. They induce a strong vertical shear, resulting in near-zero zonal mass transport in the temperature mixed layer. These observed features are in fair agreement with simple conceptual models.

During westerlies stronger than about 4 m s^{-1}, the upper 50 m becomes isothermal to within 0.1°C and the SST drops by 0.3–0.4°C for the duration of the bursts from 5°S to at least 2.5°N in our particular case. Assuming that this cooling occurs over 10°–30° longitude, it may have an appreciable impact on air-sea interactions of climatic significance [*Palmer and Mansfield*, 1984]. In contrast to the drastic near-surface salinity changes O(1 psu) observed in response to westerly bursts in November 1989 [*McPhaden et al.*, 1992], salinity around the equator was found to be only weakly affected O(0.2 psu) in February–April 1991. Origins of such a difference remain elusive, given our present inability to quantify the causative mechanisms for salinity variations using available data.

Theoretical considerations and modeling studies suggest that eastward propagating Kelvin waves in response to westerly winds may induce eastern SST warming through zonal advection of horizontal temperature gradient and/or inhibition of vertical entrainment of cold water to the surface. At present, there is ample evidence for first-baroclinic-mode equatorial Kelvin waves, identified by both their phase propagation and their meridional structure [e.g., *Delcroix et al.*, 1991*b*]. However, the expected SST warming in the eastern Pacific has yet to be detected unambiguously in observational data [*McPhaden et al.*, 1988; *Hayes et al.*, 1991]. Besides, the ability of models to successfully forecast El Niños appears closely related to low-frequency, large-scale evolution of the atmospheric circulation, i.e., independently of high-frequency events such as WWB [*Barnett et al.*, 1988]. The precise way WWB over the western Pacific warm pool actually extend their influence to lower-frequency climate fluctuations thus remains to be elucidated. In this regard, it is hoped that results from the TOGA COARE program will lead to more definitive conclusions.

Acknowledgments. We acknowledge the excellent work performed by the captain and crews of the R/V *Le Noroit* during the Alize 2 and Surtropac 14 cruises. We are most thankful to ORSTOM, IFREMER, INSU, LODYC, and the U.S. TOGA Project Office for supporting the collection and analysis of the data presented in this paper. The Florida State University wind field was kindly supplied by J. O'Brien and collaborators.

References

Bahr, F., E. Firing, and J. Songnian, Acoustic Doppler current profiling in the western Pacific during the US-PRC TOGA cruises 2, 3, and 4, *JIMAR Data Rep. 5*, 199 pp., Univ. of Hawaii, Honolulu, 1989.

Barnett, T., N. Graham, M. Cane, S. Zebiak, S. Dolan, J. O'Brien, and D. Legler, On the prediction of the El Niño of 1986–87, *Science*, *241*, 192–196, 1988.

Delcroix, T., G. Eldin, and C. Hénin, Upper ocean water masses and transports in the western tropical Pacific, *J. Phys. Oceanogr.*, *17*, 2248–2262, 1987.

Delcroix, T., F. Gallois, F. Masia, and P. Waigna, Rapport de la campagne SURTROPAC 14 à bord du N/O *Le Noroit* (11 mars au 8 avril 1991, de 20°S à 8°N le long du méridien 165°E), *Rapp. Sci. Tech. Ser. Sci. Mer Océanogr. Phys. 4*, 117 pp., Centre ORSTOM de Nouméa, Nouméa, New Caledonia, 1991*a*.

Delcroix, T., J. Picaut, and G. Eldin, Equatorial Kelvin and Rossby waves evidenced in the Pacific ocean through Geosat sea level and surface current anomalies, *J. Geophys. Res.*, *96*, 3249–3262, 1991*b*.

Delcroix, T., G. Eldin, M. H. Radenac, J. Toole, and E. Firing, Variations of the western equatorial Pacific Ocean, 1986–1988, *J. Geophys. Res.*, *97*, 5423–5445, 1992.

Eldin, G., On austral summer surface eastward flows at the equator in the western Pacific, *Proc. U.S. TOGA Western Pacific Workshop, U.S. TOGA 8*, 177–182, 1987.

Eldin, G., Coupes verticales des structures océaniques physiques à 165°E observées au cours des dix campagnes SURTROPAC, 1984–1988, *Rapp. Sci. Tech. Ser. Sci. Mer Océanogr. Phys. 1*, 130 pp., Centre ORSTOM de Nouméa, Nouméa, New Caledonia, 1989.

Eldin, G., Des Açores à la Nouvelle Calédonie, un demi-tour du monde de mesures avec un profileur acoustique à effet Doppler, *Rapp. Sci. Tech. Ser. Sci. Mer Océanogr. Phys. 3*, 59 pp., Centre ORSTOM de Nouméa, Nouméa, New Caledonia, 1991.

Eldin, G., A. Morlière, and G. Reverdin, Acoustic Doppler current profiling along the Pacific equator from 95°W to 165°E, *Geophys. Res. Lett.*, *19*, 913–916, 1992.

Feng, Y., H. P. Freitag, M. J. McPhaden, and A. J. Shepherd, Wind, current and temperature data at 0°–165°E: January 1986 to March 1991, *NOAA Data Rep. ERL PMEL-36*, 54 pp., U.S. Dept. of Commer., Washington, D. C., 1991.

Giese, B., and D. Harrison, Aspects of the Kelvin wave response to episodic wind forcing, *J. Geophys. Res.*, *95*, 7289–7312, 1990.

Gill, A., The equatorial current in an homogeneous ocean, *Deep Sea Res.*, *18*, 421–431, 1971.

Goldenberg, S., and J. O'Brien, Time and space variability of tropical Pacific wind stress, *Mon. Weather Rev.*, *109*, 1190–1207, 1981.

Grelet, J., B. Buisson, and C. Hénin, Installation et utilisation d'un thermosalinographe à bord d'un navire marchand, *Notes Tech. Ser. Sci. Mer Océanogr. Phys.*, *7*, 99 pp., Centre ORSTOM de Nouméa, Nouméa, New Caledonia, 1992.

Harrison, D., and B. Giese, Episodes of surface westerly winds as observed from islands in the western tropical Pacific, *J. Geophys. Res.*, *96*, 3221–3237, 1991.

Harrison, D., and P. Schopf, Kelvin wave-induced advection and the onset of sea surface temperature warming in El Niño events, *Mon. Westher Rev.*, *112*, 923–933, 1984.

Hayes, S., P. Chang, and M. McPhaden, Variability of the sea surface temperature in the eastern equatorial Pacific during 1986–1988, *J. Geophys. Res.*, *96*, 10,553–10,566, 1991.

Hisard, P., J. Merle, and B. Voituriez, The equatorial undercurrent at 170°E in March and April 1967, *J. Mar. Res.*, *28*, 281–303, 1970.

Istoshin, Y., and A. Kalashnikov, The Cromwell current in the western part of the Pacific, *Oceanology*, *5*, 14–16, 1965.

Keen, R., The role of cross-equatorial tropical cyclone pairs in the Southern Oscillation, *Mon. Weather Rev.*, *110*, 1405–1416, 1982.

Levitus, S., Climatological atlas of the world ocean, *NOAA Prof. Pap. 13*, 173 pp., U.S. Govt. Print. Off., Washington, D. C., 1982.

Lukas, R., and E. Londström, The mixed layer of the western equatorial Pacific ocean, *J. Geophys. Res.*, *96*, 3343–3357, 1991.

Luther, D., D. Harrison, and R. Knox, Zonal winds in the central equatorial Pacific and the onset of El Nino, *Science*, *222*, 327–330, 1983.

McCreary, J., Modelling equatorial ocean circulation, *Annu. Rev. Fluid Mech.*, *17*, 359–409, 1985.

McPhaden, M., and S. Hayes, On the variability of winds, sea surface temperature and surface layer heat content in the western equatorial Pacific, *J. Geophys. Res.*, *96*, 3331–3343, 1991.

McPhaden, M., P. Freitag, S. Hayes, B. Taft, Z. Chen, and K. Wyrtki, The response of the equatorial Pacific ocean to a westerly wind burst in May 1986, *J. Geophys. Res.*, *93*, 10,589–10,603, 1988.

McPhaden, M., S. Hayes, L. Mangum, and J. Toole, Variability in the western equatorial Pacific Ocean during the 1986–87, El Niño/Southern Oscillation event, *J. Phys. Oceanogr.*, *20*, 190–208, 1990.

McPhaden, M., F. Bahr, Y. duPenhoat, E. Firing, S. Hayes, P. Niiler, P. Richardson, and J. Toole, The response of the western equatorial Pacific ocean to westerly wind bursts during November 1989 to January 1990, *J. Geophys. Res.*, *971*, 14,289–14,303, 1992.

Meyers, G., J. R. Donguy, and R. K. Reed, Evaporative cooling of the western equatorial Pacific Ocean by anomalous winds, *Nature*, *323*, 523–526, 1986.

Palmer, T., and D. A. Mansfield, Response of two atmospheric general circulation models to sea-surface temperature anomalies in the tropical east and west Pacific, *Nature*, *310*, 483–485, 1984.

Philander, G., The response of equatorial oceans to a relaxation of the trade winds, *J. Phys. Oceanogr.*, *11*, 176–189, 1981.

Rasmusson, E., and D. Carpenter, Variations in tropical sea surface temperature and surface wind fields associated with the southern oscillation/El Niño, *Mon. Weather Rev.*, *110*, 354–384, 1982.

Reverdin, G., A. Morlière, and G. Eldin, Alize 2, campagne océanographique trans-Pacifique (janvier-mars 1991), *Rapp. Interne LODYC 91-13*, 341 pp., Université P. et M. Curie, Paris, 1991.

Stommel, H., Wind drift near the equator, *Deep Sea Res.*, *6*, 298–302, 1960.

World Climate Research Program, Scientific plan for the TOGA Coupled Ocean-Atmosphere Response Experiment, *WCRP Pub. Ser. 3*, addendum, World Meteorol. Organ., Geneva, 1990.

Wyrtki, K., El Niño—The dynamic response of the equatorial Pacific Ocean to atmospheric forcing, *J. Phys. Oceanogr.*, *5*, 572–584, 1975.

Wyrtki, K., and G. Meyers, The trade wind field over the Pacific Ocean, *J. Appl. Meteorol. 15*, 698–704, 1976.

Yoshida, S., H. Nitani, and N. Suzuki, Report of multiple ship survey in the equatorial region (International Geophysical Year), January–February 1958 (in Japanese), *Hydrol. Bull.*, *59*, 1–30, 1959.

T. Delcroix and G. Eldin, Groupe Surtropac, Centre ORSTOM de Nouméa, B.P. A5, Nouméa, New Caledonia.

M. McPhaden, NOAA PMEL, 7600 Sand Point Way NE, Seattle, WA 98115.

A. Morlière, ORSTOM/LODYC, Université Pierre et Marie Curie, 4 place Jussieu, 75252 Paris Cedex 05, France.

(Received September 17, 1992;
revised February 3, 1993;
accepted April 8, 1993.)